Prostate Cancer

Elucidating Prostate Cancer Behaviour During Treatment via Low-pass Whole-genome Sequencing of Circulating Tumour DNA

Semini Sumanasuriya [a,b,†], *George Seed* [a,†], *Harry Parr* [a], *Rossitza Christova* [a], *Lorna Pope* [a], *Claudia Bertan* [a], *Diletta Bianchini* [a,b], *Pasquale Rescigno* [a,b], *Ines Figueiredo* [a], *Jane Goodall* [a], *Gemma Fowler* [a], *Penelope Flohr* [a], *Niven Mehra* [a,b], *Antje Neeb* [a], *Jan Rekowski* [a], *Mario Eisenberger* [c], *Oliver Sartor* [d], *Stéphane Oudard* [e], *Christine Geffriaud-Ricouard* [f], *Ayse Ozatilgan* [f], *Mustapha Chadjaa* [f], *Sandrine Macé* [f], *Chris Lord* [g], *Joe Baxter* [g], *Stephen Pettitt* [g], *Maryou Lambros* [a,b], *Adam Sharp* [a,b], *Joaquin Mateo* [h], *Suzanne Carreira* [a,b], *Wei Yuan* [a,b], *Johann S. de Bono* [a,b,*]

[a] The Institute of Cancer Research, University of London, London, UK; [b] The Royal Marsden Hospital, London, UK; [c] Johns Hopkins University, Baltimore, MD, USA; [d] Tulane Medical School, New Orleans, LA, USA; [e] Hôpital Européen Georges Pompidou and Université de Paris, Paris, France; [f] Sanofi-Genzyme, Paris, France; [g] The CRUK Gene Function Laboratory and Breast Cancer Now Research Centre, The Institute of Cancer Research, London, UK; [h] Vall d'Hebron Institute of Oncology, Barcelona, Spain

Article info

Abstract

Background: Better blood tests to elucidate the behaviour of metastatic castration-resistant prostate cancer (mCRPC) are urgently needed to drive therapeutic decisions. Plasma cell-free DNA (cfDNA) comprises normal and circulating tumour DNA (ctDNA). Low-pass whole-genome sequencing (lpWGS) of ctDNA can provide information on mCRPC behaviour.

Objective: To validate and clinically qualify plasma lpWGS for mCRPC.

Design, setting, and participants: Plasma lpWGS data were obtained for mCRPC patients consenting to optional substudies of two prospective phase 3 trials (FIRSTANA and PROSELICA). In FIRSTANA, chemotherapy-naïve patients were randomised to treatment with docetaxel (75 mg/m^2) or cabazitaxel (20 or 25 mg/m^2). In PROSELICA, patients previously treated with docetaxel were randomised to 20 or 25 mg/m^2 cabazitaxel. lpWGS data were generated from 540 samples from 188 mCRPC patients acquired at four different time points (screening, cycle 1, cycle 4, and end of study).

Outcome measurements and statistical analysis: lpWGS data for ctDNA were evaluated for prognostic, response, and tumour genomic measures. Associations with response and survival data were determined for tumour fraction. Genomic biomarkers including large-scale transition (LST) scores were explored in the context of prior treatments.

Results and limitations: Plasma tumour fraction was prognostic for overall survival in univariable and stratified multivariable analyses (hazard ratio 1.75, 95% confidence interval 1.08–2.85; *p* = 0.024) and offered added value compared to existing biomarkers (C index 0.722 vs 0.709; *p* = 0.021). Longitudinal changes were associated with drug response. PROSELICA samples were enriched for LSTs (*p* = 0.029) indicating genomic instability, and this enrichment was associated with prior abiraterone and enzalutamide

[†] These authors contributed equally to this work and are joint lead authors.
[*] Corresponding author. The Institute of Cancer Research, 15 Cotswold Road, London SM2 5NG, UK. Tel. +44 208 7224029; Fax: +44 208 6427979.
E-mail address: johann.de-bono@icr.ac.uk (J.S. de Bono).

treatment but not taxane or radiation therapy. Higher LSTs were correlated with losses of *RB1/RNASEH2B*, independent of *BRCA2* loss.

Conclusions: Plasma lpWGS of ctDNA describes CRPC behaviour, providing prognostic and response data of clinical relevance. The added prognostic value of the ctDNA fraction over established biomarkers should be studied further.

Patient summary: We studied tumour DNA in blood samples from patients with prostate cancer. We found that levels of tumour DNA in blood were indicative of disease prognosis, and that changes after treatment could be detected. We also observed a "genetic scar" in the results that was associated with certain previous treatments. This test allows an assessment of tumour activity that can complement existing tests, offer insights into drug response, and detect clinically relevant genetic changes.

1. Introduction

Prostate cancer (PC) remains a major cause of male cancer deaths [1] despite significant advances in systemic treatment [2]. Taxanes improve overall survival (OS) and provide symptomatic benefit from metastatic castration-resistant PC (mCRPC) [3,4] but uncertainty remains regarding how long to continue treatment, with early prostate-specific antigen (PSA) changes unable to guide treatment switch decisions. Better biomarkers of response are needed for early discontinuation of ineffective treatment. Measurement of total circulating cell-free DNA (cfDNA) in serial plasma samples is prognostic but is challenged by nonmalignant circulating DNA. The fraction of cfDNA that is tumour-derived—circulating tumour DNA (ctDNA)—can be estimated via next-generation sequencing to generate quantitative [5] and qualitative data [6], with serial ctDNA genomics providing important insights into disease behaviour and evolution [7].

Low-pass whole-genome sequencing (lpWGS) assesses genome-wide copy number events [8], allowing rapid, high-throughput, inexpensive testing of ctDNA and estimation of cfDNA tumour fraction, ploidy, and whole-genome copy number alterations (CNAs). lpWGS can characterise the impact of DNA repair defects and genomic instability by detailing copy-number fragment size and frequency, including large-scale transitions (LSTs) and tandem duplications [9–11]. Homologous repair scores, to which LSTs contribute, have been linked to PARP inhibitor sensitivity, and tandem duplication CNA genotypes reflect deleterious *CDK12* alterations that sensitise the individual to immunotherapy [10,12].

We validated a cfDNA lpWGS assay and tested samples from mCRPC patients treated in two taxane phase 3 trials, FIRSTANA (NCT01308567) and PROSELICA (NCT01308580). In FIRSTANA, chemotherapy-naïve patients were randomised to docetaxel (75 mg/m^2) or cabazitaxel (20 or 25 mg/m^2); in PROSELICA, docetaxel-pretreated patients were randomised to 20 or 25 mg/m^2 cabazitaxel [13,14]. Here we present lpWGS data from patients consenting to these extra analyses and clinical qualification that this biomarker provides prognostic and response data as well as information on evolving progressing disease.

2. Patients and methods

2.1. Patients and sample collection

Supplementary Figure 1 shows an outline of our study, while Supplementary Figure 2A,B shows overviews of the FIRSTANA and PROSELICA trials. Both trials have already been reported [13–15]. OS was defined as the time from randomisation to death from any cause. Patients who did not have an event were censored at the date of last contact. Radiographic and PSA progression-free survival (rPFS and PSA-PFS) were defined as the time from randomisation to the date of tumour progression.

To determine progression and response status we used Response Evaluation Criteria in Solid Tumours 1.1 and Prostate Cancer Working Group 2 Criteria, as previously described in the FIRSTANA and PROSELICA reports [13–15]. Studies on ctDNA were prospectively included as an optional exploratory endpoint in both trials. Clinical data included PSA, lactate dehydrogenase, haemoglobin, serum albumin, alkaline phosphatase, and Eastern Cooperative Oncology Group performance status. Plasma was collected from patients consenting to this substudy at two baseline time points 1–4 wk apart (at screening [SCR] and cycle 1 day 1 [C1]) and at cycle 4 day 1 (C4) and at the end of the study (EOS). Blood was collected in lithium heparin tubes (BD Vacutainer; BD Biosciences, San Jose, CA, USA). Plasma was collected from healthy volunteers (n = 10) and pooled prior to lpWGS. Biopsies were collected according to a prospective PC molecular characterisation protocol approved by the institutional review board [16].

2.2. cfDNA extraction and quantification

cfDNA was isolated from 1–4 ml of plasma using a QIAamp Circulating Nucleic Acid kit (Qiagen, Hilden, Germany). Of the 60 μl of eluate, 3 μl was used for quantification via a Quant-IT Picogreen HS DNA kit (ThermoFisher, Waltham, MA, USA) and concentrations were read on a BioTek microplate spectrophotometer (excitation 480 nm, emission 520 nm) (BioTek Instruments, Winooski, VT, USA).

2.3. Library preparation and sequencing

Following extraction, samples were treated with heparinase I (Sigma-Aldrich, St. Louis, MO, USA) [17]. Low-pass whole-genome library preparation was carried out using a Qiagen QiaSeq FX DNA library kit (Qiagen). Samples were sequenced on an Illumina NovaSeq 6000 platform (Illumina, San Diego, CA, USA). Technical replicates were prepared and sequenced on an Illumina MiSeq system (Illumina) [18].

2.4. Bioinformatics processing

lpWGS data were converted to paired-end reads (bcl2fastq2 v.2.17.1.14) with default settings and subsequently aligned to the human reference genome (GRCh37) using the BWA-MEM (version 0.7.12) algorithm [33]. Quality control checks were performed using Picard (Broad Institute, Cambridge, MA, USA, version 2.8.1) and FASTQC (Babraham Institute, Babraham, UK, version 0.11.8). Samples were excluded from analysis if the sequencing depth was less than $0.05\times$ or if they failed the FASTQC read quality filter. Aligned reads were quantified using HMMcopy readCounter [35] (version 0.99.0) with the quality filter and interval width set to 20 and 500 kb, respectively.

Read depth data were modelled and the tumour fraction was calculated using ichorCNA (version 0.1.0) [19]. Transition strength parameters were set at –txnE = 0.99999 and –txnStrength = 100000; the maximum copy number (CN) was set to 20 to account for amplifications. The germline DNA fraction (initial values 40% and 90%), ploidy (initial values 2 and 3), and subclonality were modelled. The default 500-kb reference coverage data set supplied with ichorCNA was used.

2.5. Data handling and statistical analyses

IchorCNA provides segmented CN data and estimates of tumour fraction and ploidy. These were further processed to generate both CN calls and LST values, as described in the Supplementary material [20]. Cox proportional-hazards models were used for multivariable survival analysis, and Kaplan-Meier curves for univariable survival comparisons.

The log-likelihood test was used to compare regression models. Multivariable generalised linear and logistic regressions were used to study continuous and binary outcomes, respectively. A full listing of the regression variables is provided in the Supplementary material. Comparisons of continuous variables (tumour fraction and LST scores) between groups (study subset, prior treatment, specific CN events) in violin plots used the Wilcoxon rank-sum (unpaired data) or signed-rank (paired data) tests. Elastic-net regression was performed using eNetXplorer (version 1.1.0) [21], for which parameter selections are presented in the Supplementary material. Following elastic-net regression, significant ($p < 0.05$) bins were merged with adjacent highly correlated (Pearson's $r > 0.9$) bins to form merged regions for subsequent analyses, with the CN values of the most significant overlapping bin assigned to each final merged region.

3. Results

3.1. FIRSTANA and PROSELICA cohorts providing plasma samples for lpWGS

lpWGS data were generated from 540 samples acquired at four time points (SCR and C1, representing baseline, and C4 and EOS). Samples with plasma available after other preplanned analyses were tested, including 299 FIRSTANA (104 SCR, 55 C1, 79 C4, and 61 EOS) and 241 PROSELICA (84 SCR, 34 C1, 59 C4, and 64 EOS) samples. The

Table 1 – Baseline characteristics of the cohorts with castration-resistant prostate cancer from the FIRSTANA and PROSELICA studies

Characteristic	FIRSTANA (n = 103)	PROSELICA (n = 85)	p value
ECOG PS ≥2, n (%) [b]	3 (2.9)	10 (12)	0.02 [a]
RECIST-measurable, n (%) [b]	54 (52)	45 (53)	0.9 [a]
Visceral disease, n (%)	20 (19)	25 (29)	0.11 [a]
Pain at baseline, n (%) [c]	69 (67)	59 (69)	0.4 [a]
Gleason score <8 at diagnosis, n (%) [d]	42 (41)	45 (53)	0.051 [a]
Prior Abi/Enza treatment, n (%)	2 (1.9)	29 (35)	<0.001 [a]
Trial arm, n (%)			
Cabazitaxel (20 mg/m²)	34 (33)	41 (48)	
Cabazitaxel (25 mg/m²)	28 (27)	44 (52)	
Docetaxel (75 mg/m²)	41 (40)	0 (0)	
Median age, yr (IQR)	68.0 (62.5–72.0)	67 (64.0–71.0)	0.2 [e]
Median LDH, U/l (IQR)	267 (204–360)	366 (234–605)	0.003 [e]
Median ALP, U/l (IQR)	129 (81.0–242)	214 (118–413)	0.002 [e]
Median haemoglobin, g/dl (IQR)	121 (111–128)	112 (105–122)	<0.001 [e]
Median albumin, g/dl (IQR)	40.2 (37.5–43.4)	40.0 (36.0–43.0)	0.2 [e]
Median PSA, ng/ml (IQR)	60.4 (18.2–188)	161 (64.9–623)	<0.001 [e]
Median PSA doubling time, d (IQR)	62 (36–100)	51 (35–86)	0.3 [e]
Median NLR (IQR)	2.25 (1.53–4.10)	2.79 (1.69–3.89)	0.17 [e]
Outcomes			
>50% PSA response at 12 wk, n (%)	55 (53)	23 (27)	<0.001 [a]
>50% PSA response at any time, n (%)	68 (66)	33 (39)	<0.001 [a]
Median OS, mo (95% CI)	21.3 (17.2–23.9)	13.3 (11.5–15.8)	<0.001 [f]
Median rPFS, mo (95% CI)	11.6 (9.86–13.6)	7.13 (6.11–12.4)	0.003 [f]
Median PSA-PFS, mo (95% CI)	7.43 (6.64–8.94)	4.86 (4.14–7.29)	0.003 [f]
Censored (n)	30	6	
Median FU for censored patients (mo)	32.0	Insufficient cases	

Abi = abiraterone; ALP = alkaline phosphatase; ECOG PS = Eastern Cooperative Oncology Group performance status; Enza = enalutamide; FU = follow-up; IQR = interquartile range; LDH = lactate dehydrogenase; NLR = neutrophil/lymphocyte ratio; OS = overall survival; PFS = progression-free survival; PSA = prostate-specific antigen; RECIST = Response Evaluation Criteria in Solid Tumours; rPFS = radiographic PFS.
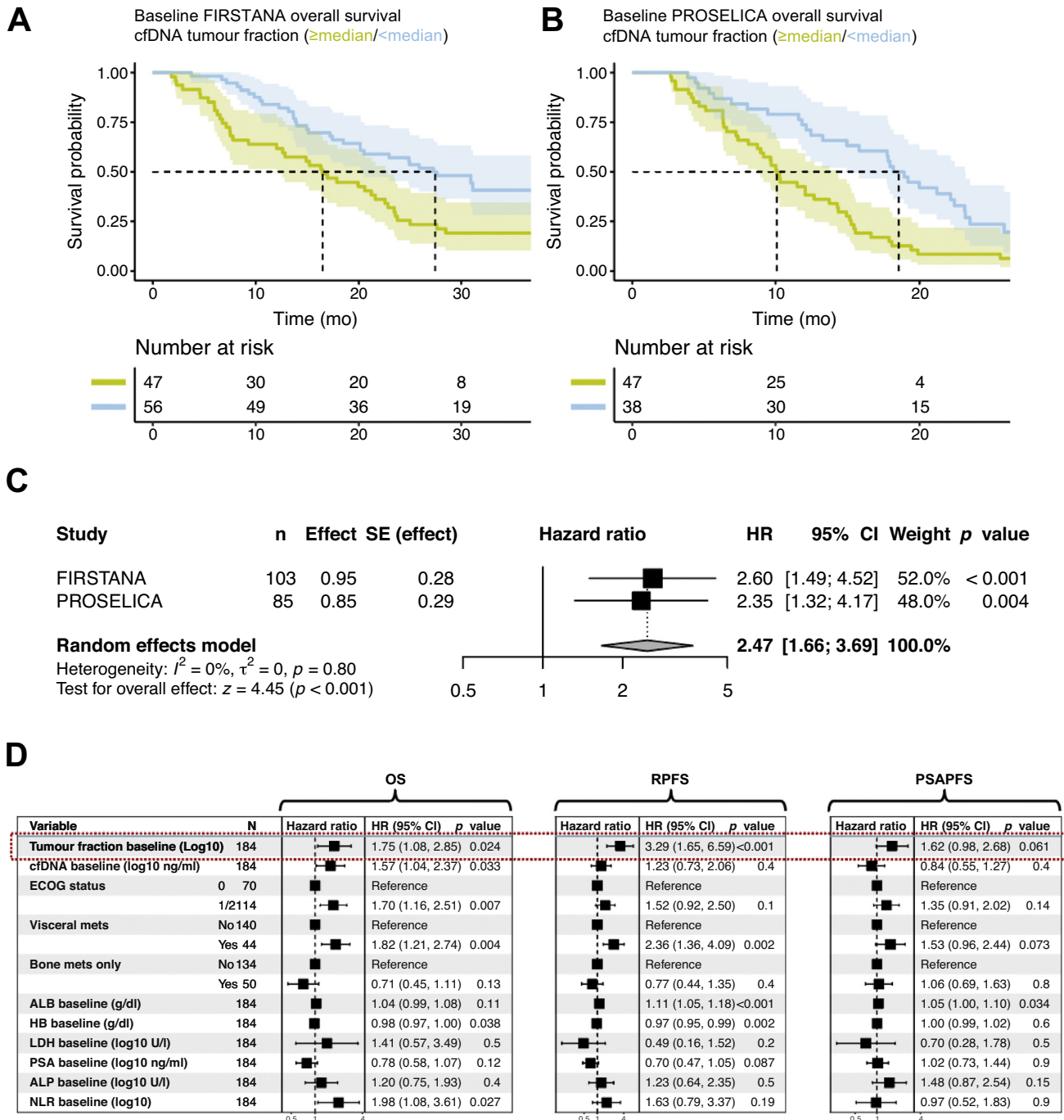[a] χ^2 test.
[b] Stratification parameters.
[c] Twenty assessments missing (15 in FIRSTANA and 5 in PROSELICA).
[d] Twelve assessments missing (5 in FIRSTANA and 7 in PROSELICA).
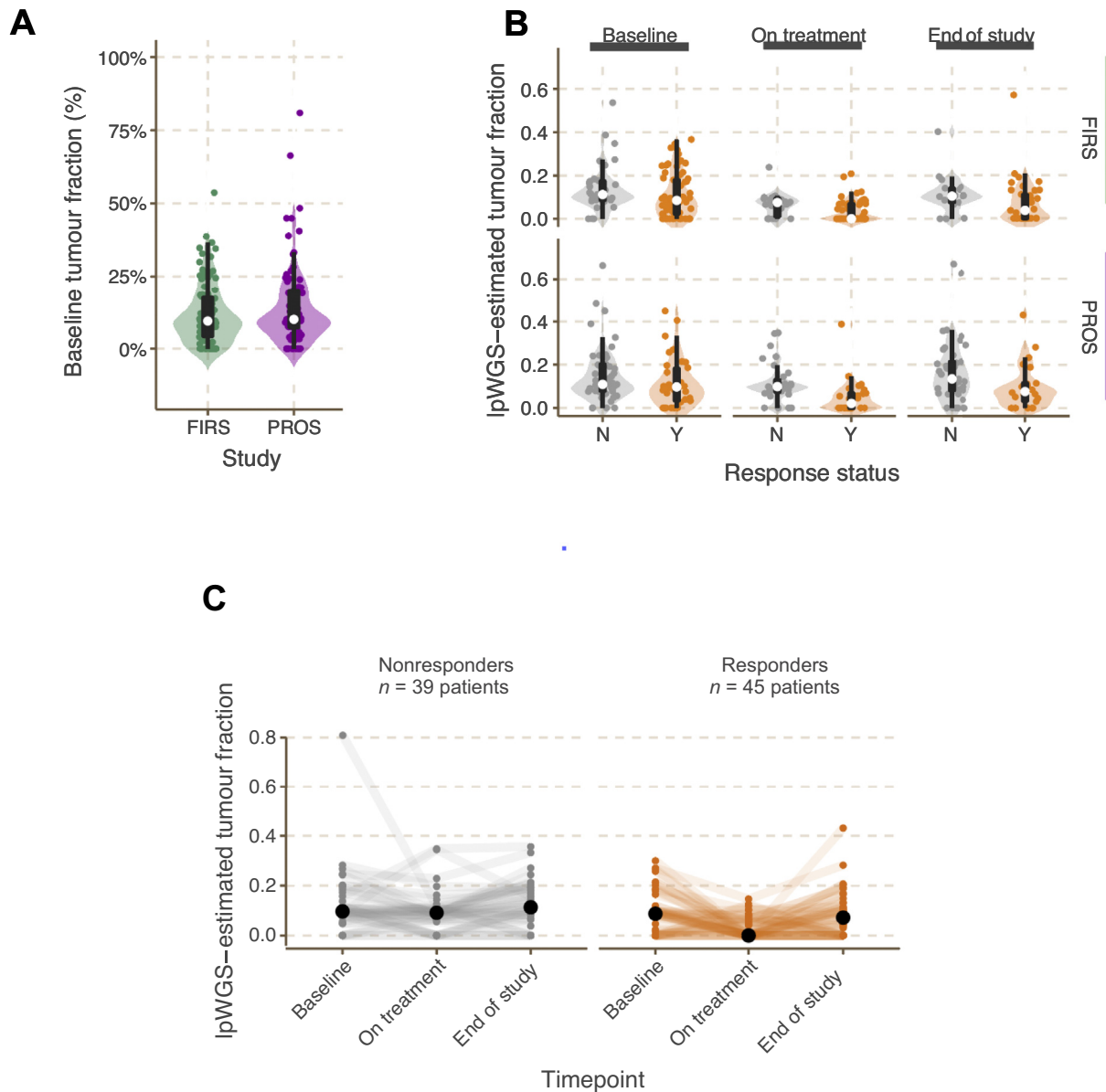[e] Wilcoxon rank-sum test.
[f] Log-rank test.

Fig. 1 – Cell-free DNA (cfDNA) tumour fraction estimates are prognostic. (A,B) Univariable analysis of overall survival (OS) with cohort stratification by median baseline tumour fraction (average for the screening and cycle 1 day 1 samples; yellow = high, blue = low) across the (A) FIRSTANA (discovery) and (B) PROSELICA (validation) cohorts. Kaplan-Meier plots with confidence intervals (CIs) and matching risk tables are shown. Dashed lines indicate the time to 50% survival. (C) Univariable regression random-effects meta-analysis of OS by cfDNA tumour fraction (continuous variable, $\log_{10}$ transformed) in the FIRSTANA (discovery) and PROSELICA (validation) cohorts. Effect size, hazard ratio (HR), 95% CI, and p values for the overall test for effect are shown. SE = standard error. (D) Forest plots showing multivariable analysis of OS, radiographic progression-free survival (RPFS) and PSA progression-free survival (PSAPFS) from Cox proportional-hazards models. Statistical models were stratified by study inclusion (FIRSTANA vs PROSELICA) because of underlying differences in survival. The median baseline tumour fraction (continuous variable, $\log_{10}$-transformed) and median baseline cfDNA total concentration (continuous variable, log10-transformed) are included in the model, along with other baseline clinical variables prognostic for mCRPC.
ECOG = Eastern Cooperative Oncology Group; Mets = metastases; ALB = albumin; HB = haemoglobin; LDH = lactate dehydrogenase; PSA = prostate-specific antigen; ALP = alkaline phosphatase; NLR = neutrophil/lymphocyte ratio.

characteristics for the 188 patients involved are presented in Table 1 (FIRSTANA $n = 103$ and PROSELICA $n = 85$; Supplementary Figs. 1 and 2). PROSELICA substudy patients had worse prognostic characteristics than the FIRSTANA group, in keeping with a more heavily pretreated cohort. Only <2% FIRSTANA substudy patients received abirater-

one/enzalutamide, in contrast to 34% of PROSELICA substudy patients. The PSA response rate was lower in PROSELICA than in FIRSTANA (39% vs 66%), similar to previous reports [5,13,14]. The baseline clinical and survival characteristics of these cohorts compared to the overall trial populations are described in Supplementary

Fig. 2 – Treatment-induced changes in the tumour fraction in cell-free DNA (cfDNA). (A) Violin plots comparing baseline tumour fraction between FIRSTANA (FIRS) and PROSELICA (PROS) plasma samples. Wilcoxon rank-sum test: $p = 0.2$. Values for the median (white point; FIRS = 0.0949, PROS = 0.101), interquartile range (IQR, black rectangle; FIRS = 0.0436 to 0.175, PROS = 0.0740 to 0.197), and 1.5 × IQR (black lines) tumour fractions are also shown. (B) Violin plots illustrating changes in tumour fraction in the unmatched cohort for patients categorised as responders (either prostate-specific antigen decrease of 50% or radiographic response) or nonresponders at multiple time points. Plots are split between FIRS and PROS cohorts. Unpaired Wilcoxon rank-sum tests yielded the following results: baseline (BL) FIRS: responder ($n = 70$, median 0.0850) versus nonresponder ($n = 33$, median 0.112), $p = 0.045$; on treatment (OT) FIRS: responder ($n = 55$, median 0) versus nonresponder ($n = 22$, median 0.0755), $p = 0.003$; end of study (EOS) FIRS: responder ($n = 39$, median 0.0365) versus nonresponder ($n = 18$, median 0.105), $p = 0.035$; BL PROS: responder ($n = 34$, median 0.0976) versus nonresponder ($n = 51$, median 0.109), $p = 0.13$; OT PROS: responder (n = 26, median 0.0213) versus nonresponder (n = 32, median 0.0991), $p < 0.001$; EOS PROS: responder ($n = 22$, median 0.0766) versus nonresponder ($n = 41$, median 0.134), $p = 0.035$. (C) Analysis of matched same-patient cfDNA sample sets showing longitudinal tumour fraction changes for nonresponders ($n = 39$) and responders ($n = 45$). Median values are in black. Lines connecting points indicate same-patient sets. Paired Wilcoxon signed-rank tests yielded the following results: nonresponder BL (median 0.0966) versus OT (median 0.091), $p = 0.06$; nonresponder BL (median 0.0966) versus EOS (median 0.113), $p = 0.17$; nonresponder OT (median 0.0912) versus EOS (median 0.113), $p = 0.006$; responder BL (median 0.0873) versus OT (median 0), $p < 0.001$; responder BL (median 0.0873) versus EOS (median 0.0718), $p = 0.2$; responder OT (median 0) versus EOS (median 0.0718), $p = 0.001$.

Table 1. Maximum follow-up across the two trials was 51 and 48 mo. No differences in response or survival were noted in the substudy cohorts compared to the overall populations.

3.2. Validation of lpWGS CNA profile acquisition

lpWGS data were generated from cfDNA samples, with median sequencing coverage of 1.9X . We identified mCRPC genomic profiles (Supplementary Fig. 3) with common events including AR (chromosome Xq) and MYC (chromosome 8q) loci (Supplementary Fig. 3A). Cases with frequent large-scale CN changes described in tumours with *BRCA1/2* loss were observed [22] (Supplementary Fig. 3B), as well as focal tandem duplication patterns linked to *CDK12* loss [10] (Supplementary Fig. 3C). The overall CNA profile of our cohort was consistent with previously published mCRPC biopsy data [23] (Supplementary Fig. 3D).

To evaluate lpWGS CNA sensitivity, we used a baseline sample with an estimated tumour fraction of 50% and serially diluted it with pooled healthy volunteer cfDNA. The diluted profiles closely matched each other, but estimation of absolute CNA values was challenging when the tumour fraction was <5% (Supplementary Fig. 4A) [19]. cfDNA tumour fractions estimated via lpWGS were consistent with the expected fractions following dilution (Pearson's r = 0.994; Supplementary Fig. 4B). We further studied technical and biological replicates; ten samples subjected to duplicate library preparations showed highly correlated CNA profiles (Pearson's r = 0.948; Supplementary Fig. 4C). Biological replicates (same-patient samples taken 1–4 wk apart at SCR and C1, n = 88) showed reproducible CNAs (Supplementary Fig. 5A) and tumour fractions (Supplementary Fig. 5B).

3.3. Baseline cfDNA tumour fraction and prognosis

To explore univariable associations, we split the entire FIRSTANA + PROSELICA lpWGS cohort according to the overall median baseline ctDNA fraction, which was 9.6% (Fig. 1A). High baseline ctDNA fraction was correlated with shorter OS in the FIRSTANA and PROSELICA trials, with 10-mo-shorter median OS (Fig. 1A,B). Analysis of the tumour fraction as a continuous variable in FIRSTANA and PROSELICA independently and collectively confirmed these findings (Cox proportional-hazard models, $p < 0.001$ and $p = 0.004$; meta-analysis test for overall effect, $p < 0.001$; Fig. 1C). The baseline ctDNA fraction was also significantly associated with rPFS and PSA-PFS (Supplementary Fig. 6). The relationship between detectable ctDNA fraction (present/absent) on treatment and OS is shown in Supplementary Figure 7. Furthermore, the baseline ctDNA fraction was associated with several other clinical variables (Supplementary Fig. 8).

We applied a multivariable Cox proportional-hazards model, as described in the Supplementary material, to investigate OS, rPFS, and PSA-PFS (n = 184 of 188 patients with complete data) and, importantly, stratified by study

inclusion (Fig. 1D) [5]. The baseline ctDNA fraction was independently associated with worse outcomes for all three endpoints; the hazard ratio was 1.75 (95% confidence interval [CI] 1.08–2.85; $p = 0.024$) for OS, 3.29 (95% CI 1.65–6.59; $p < 0.001$) for rPFS, and 1.62 (95% CI 0.98–2.68; $p = 0.061$) for PSA-PFS. We found that inclusion of the tumour fraction in multivariable survival models led to a significant improvement (OS, C index 0.722 vs 0.709; likelihood-ratio test, $p = 0.021$; Supplementary Table 2). These data indicate that the ctDNA fraction provides independent information in the context of established clinical biomarkers.

3.4. ctDNA fraction and response to taxane treatment

There was no statistically significant difference in baseline ctDNA fraction between the FIRSTANA and PROSELICA cohorts (median 9.5% vs 10%; Wilcoxon rank-sum test, $p = 0.2$; Fig. 2A). The ctDNA fraction among nonresponding FIRSTANA patients (determined via serial radiological and PSA analyses) was relatively stable throughout treatment (median 11% at baseline, 7.5% on treatment, and 10% at EOS). By contrast, the ctDNA fraction among responders exhibited large decreases on treatment (median 8.5% at baseline, 0% on treatment, and 3.7% at EOS). These observations were replicated in the PROSELICA cohort (Fig. 2B). In keeping with these findings, CNAs became undetectable in responders while on treatment (Supplementary Fig. 9). We further evaluated the ctDNA fraction in longitudinal same-patient samples (n = 252 samples from 84 patients; Fig. 2C). Among responders, the ctDNA fraction significantly decreased on treatment (Wilcoxon signed-rank test, $p < 0.001$) and increased at EOS (median 8.7% at baseline, 0% on treatment, and 7.2% at EOS); this was not observed for nonresponders (median 9.7% at baseline, 9.1% on treatment, and 11.3% at EOS).

3.5. lpWGS provides insights into PC genomic instability

We next explored LST as a measure of genomic instability [22]. PROSELICA baseline samples exhibited a significantly higher LST score compared with FIRSTANA baseline samples (Wilcoxon rank-sum test, $p = 0.029$; Fig. 3A); however, there was no correlation between LST score and estimated tumour fraction (Supplementary Fig. 10A). We hypothesised that LST score differences could be explained by prior treatment, and found that patients who had received abiraterone or enzalutamide had significantly higher LST scores (median LST score: 18 untreated vs 26 treated; Wilcoxon rank-sum test, $p = 0.003$; Fig. 3B and Supplementary Fig. 10B). Examples of CN profiles of samples with high, intermediate, and low LST scores are shown in Supplementary Figure 10C.

This was maintained in multivariable logistic regression analysis that included other known prognostic factors (including ctDNA tumour fraction) with the LST score (odds ratio 17.2, 95% CI 1.98–223; $p = 0.018$; Fig. 3C). However, there was no significant difference in LST score between individuals pretreated with radical radiotherapy and
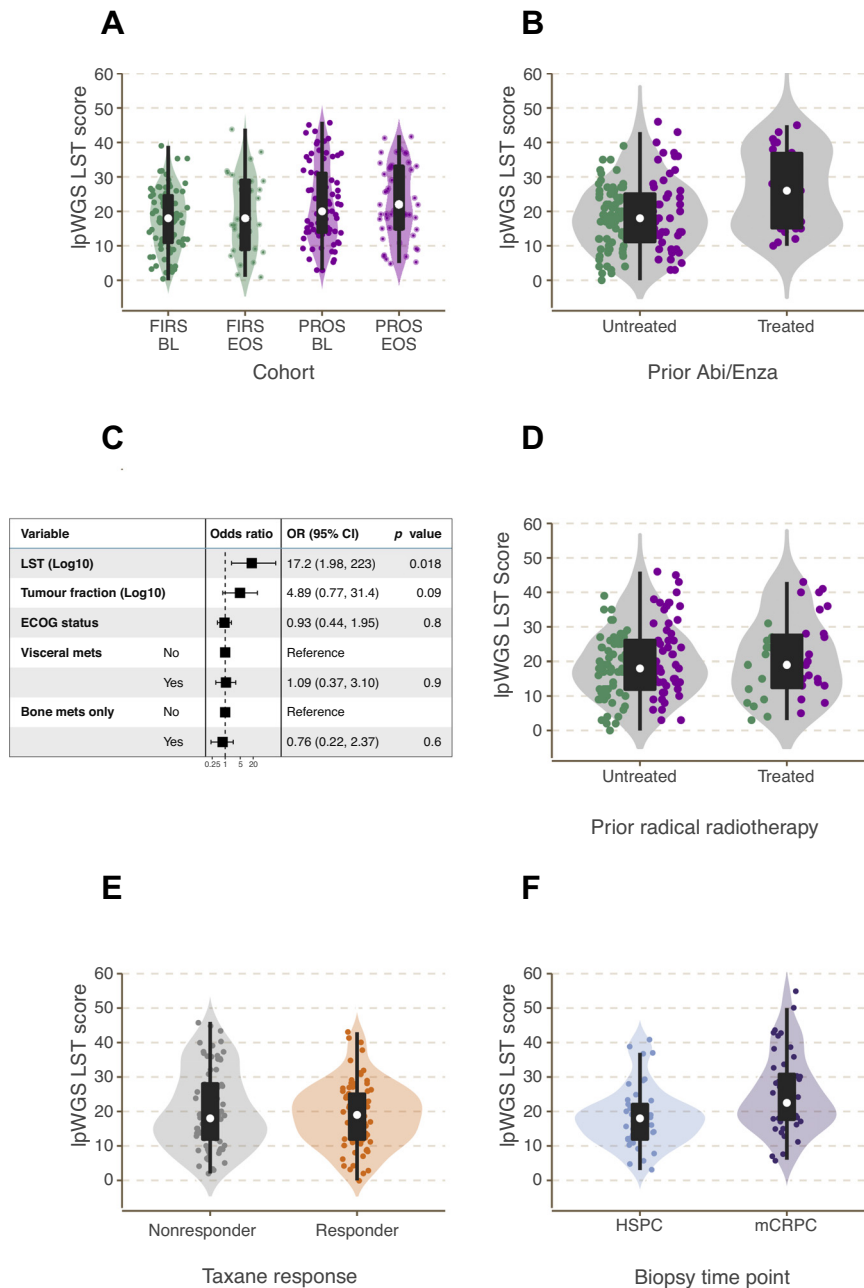
Fig. 3 – Genomic copy number burden and large-scale transition (LST) in metastatic castration-resistant prostate cancer (mCRPC). (A) Violin plot comparison of LST scores between baseline (BL) and end of study (EOS) for the FIRSTANA (FIRS) and PROSELICA (PROS) cohorts. Samples with a tumour fraction >5% were assessed; in cases with multiple BL data, the highest-fraction sample was used. Values for the median (white point), interquartile range (IQR; black rectangle) and 1.5 × IQR (black lines) LST scores are also shown. Unpaired Wilcoxon rank-sum tests yielded the following results: FIRS BL (median 18, IQR 11-24.5) versus FIRS EOS (median 18, IQR 9-29), $p = 0.5$; FIRS BL (median 18, IQR 11-24.5) versus PROS BL (median 20, IQR 14-31), $p = 0.029$; PROS BL (median 20, IQR 14-31) versus PROS EOS (median 22, IQR 15-33), $p = 0.7$. (B) Comparison of baseline LST scores between patients with prior abiraterone (Abi) or enzalutamide (Enza) exposure and untreated patients ($n = 152$). FIRSTANA patients are shown in green and PROSELICA patients in purple; after removal of cases with a low tumour fraction, no FIRSTANA patients had received Abi/Enza and a significant proportion of PROSELICA patients had received Abi/Enza. Median, IQR, and 1.5 × IQR LST scores shown as for A. Unpaired Wilcoxon rank-sum tests yielded the following results: untreated FIRS (median 18, IQR 11-24.5) versus untreated PROS (median 18, IQR 13-27.5), $p = 0.3$; overall untreated (median 18, IQR 11.2-25) versus overall treated (median 26, IQR 15.2-36.8), $p = 0.003$. (C) Forest plot of the multivariable logistic regression model for association of LST with prior Abi/Enza treatment, depicting ability of LST score to predict Abi/Enza status in the context of tumour fraction and other clinical biomarkers. (D) Comparison of baseline LST values between patients who had received prior radical radiotherapy and those who had not. FIRSTANA patients are shown in green and PROSELICA patients in purple ($n = 152$). Median, IQR, and 1.5 × IQR LST scores shown as for A. Unpaired Wilcoxon rank-sum tests yielded the following results: untreated FIRS (median 18, IQR 12-25) versus untreated PROS (median 19.5, IQR 14-31), $p = 0.10$; treated FIRS (median 17, IQR 8.25-24) versus treated PROS (median 20, IQR 14-35), $p = 0.11$; overall untreated (median 18, IQR 12-26) versus overall treated (median 19, IQR 12.5-27.5), $p = 0.8$. (E) Violin plot comparison of baseline LST scores in FIRSTANA and PROSELICA by taxane treatment response ($n = 152$). Median, IQR, and 1.5 × IQR LST scores shown as for A. A Wilcoxon rank-sum test for nonresponders (median 18, IQR 12-28) versus responders (median 19, IQR 12-25) yielded $p = 0.6$. (F) Comparison of LST scores in the validation cohort of same-patient samples (44 patients, 88 samples) between primary hormone-sensitive prostate cancer (HSPC) and mCRPC sample pairs. Median, IQR, and 1.5 × IQR LST scores shown as for A. A paired Wilcoxon rank-sum test for HSPC (median 18, IQR 12-22) versus mCRPC (median 22.5, IQR 17.8-30.8) yielded $p < 0.001$.
ECOG = Eastern Cooperative Oncology Group; Mets = metastases; OR = odds ratio; CI = confidence interval.
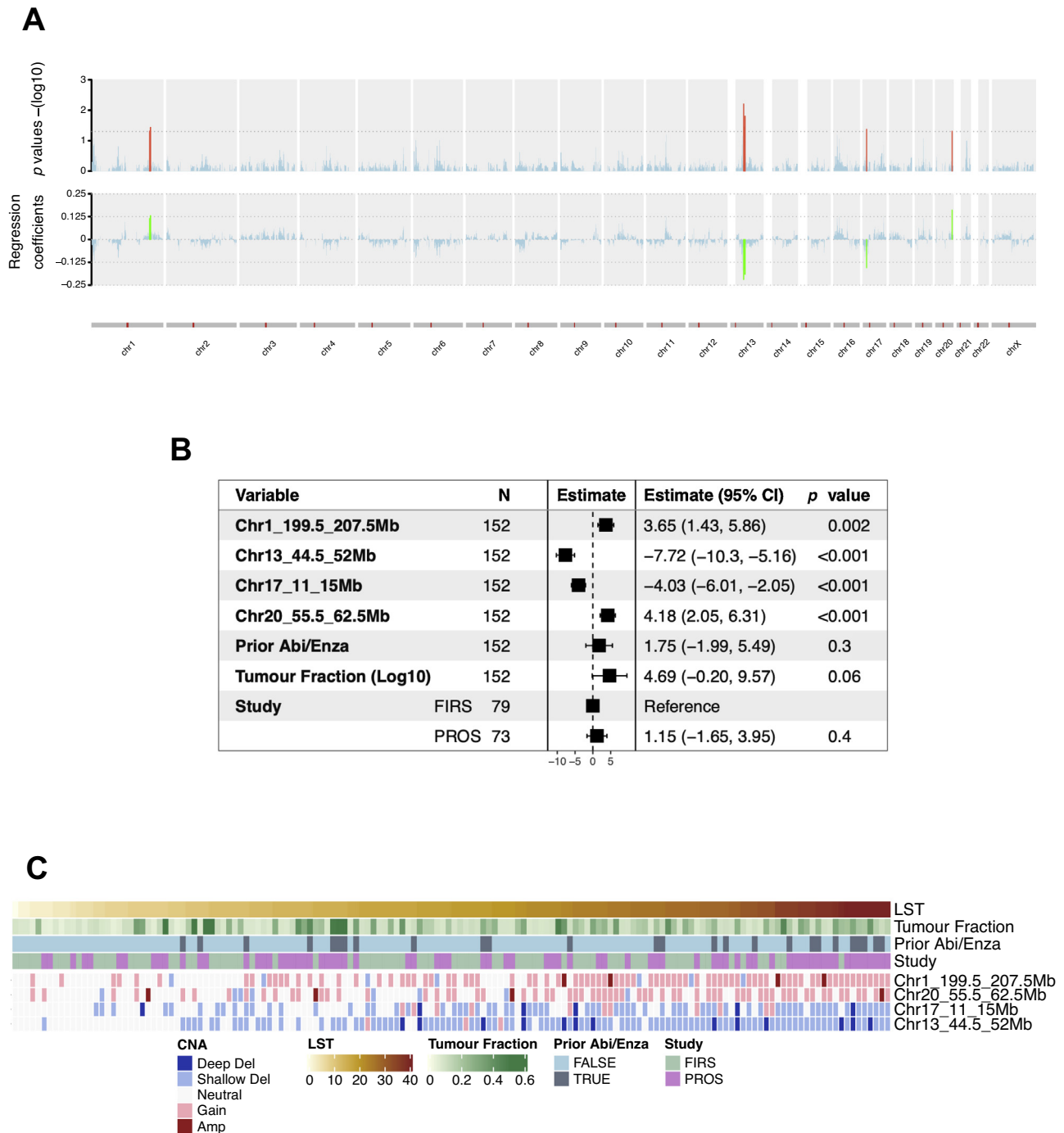
Fig. 4 – Genomic regions associated with LST. (A) Elastic-net regression model results for genome-wide copy-number alterations showing cross-validated p values (−$\log_{10}$-transformed) and regression coefficients for each 500-kb genomic bin. Loci with significant ($p < 0.05$) genomic alteration are depicted in red in the p-value plot and in green in the regression-coefficient plot. (B) Forest plot showing multivariable generalised linear model analysis of the genomic loci identified as associated with higher LST scores. Tumour fraction ($\log_{10}$-transformed), prior abiraterone (Abi) or enzalutamide (Enza) treatment, and study inclusion (FIRSTANA vs PROSELICA) were also included in the model. (C) Heatmap illustrating CNAs in regions (rows) significantly ($p < 0.05$) associated with LST scores. The samples (columns) are ordered by LST score, with additional annotation for estimated tumour fraction, prior abiraterone/enzalutamide status, and study inclusion (FIRSTANA vs PROSELICA). CNAs are coloured by type. LST = large-scale transition; CNA = copy number alteration; Del = deletion.

untreated individuals (Fig. 3D), or between taxane responders and nonresponders (Fig. 3E).

We confirmed these findings using same-patient samples from hormone-sensitive PC (diagnostic, primary tumours) and CRPC (metastatic) biopsies ($n = 88$) [16], all of whom had received abiraterone or enzalutamide before CRPC biopsy (Supplementary Table 3). LST scores increased significantly (median scores 18 and 22.5; Wilcoxon rank-sum test, $p < 0.001$) after exposure to abiraterone or enzalutamide in this cohort (Fig. 3F).
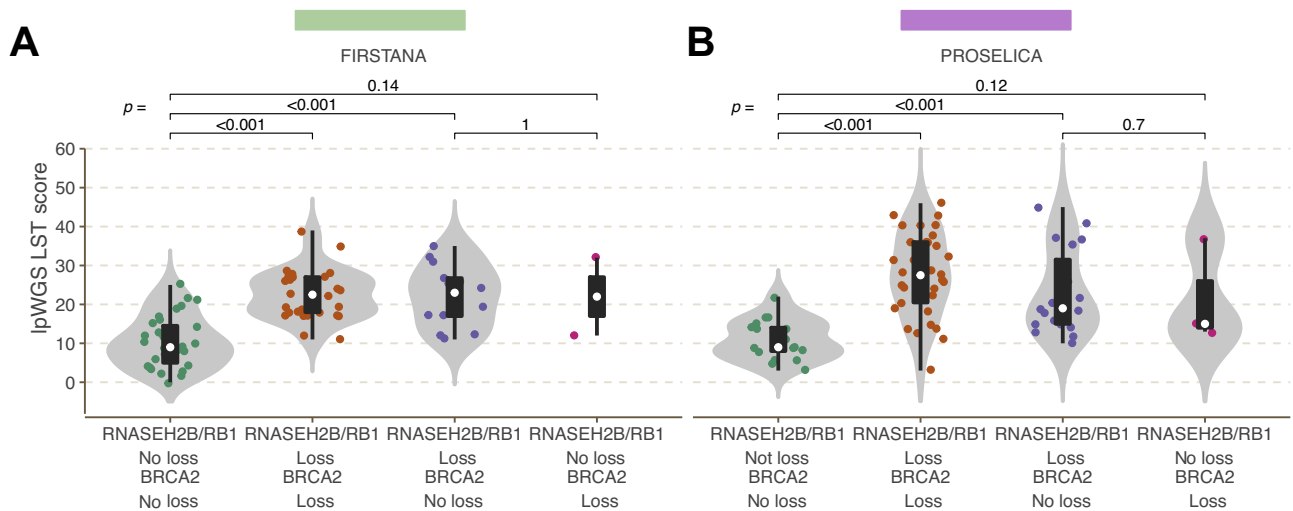
Fig. 5 – Chromosome 13 deletions and LST score. Violin plot comparisons of baseline LST scores for different chromosome 13 deletion combinations across the (A) FIRSTANA and (B) PROSELICA cohorts. Values for the median (white point), interquartile range (IQR; black rectangle), and 1.5 × IQR (black lines) LST scores are shown. The *p* values are for between-group Wilcoxon rank-sum tests.
lpWGS = low-pass whole-genome sequencing; LST = large-scale transition.

3.6. Association of LST score with tumour CNAs

To explore CNAs associated with LST scores, we performed elastic-net regression, which avoids false positives due to multiple testing. Among baseline samples, several CNAs were associated with high LST values ($p < 0.05$), the most significant of which was chromosome 13 loss (Fig. 4A). We then applied a multivariable generalised linear model to assess the association of these regions with LST score and found that loss of two regions on chromosomes 13 and 17, and gain of two regions on chromosomes 1 and 20 remained the most strongly associated with high LST scores (Fig. 4B).

Genes within these loci, with an overlap of publicly available PARP inhibitor CRISPR screen data, are detailed in the Supplementary material. Interestingly, when ranked by LST score, co-occurrence of several of the genomic loci most associated with a high LST score was evident (Fig. 4C). However, we surprisingly observed that the key loci highlighted by this multivariable approach did not point to *BRCA2*, but instead focused on the *RB1/RNASEH2B* region, although these analyses are limited by sample size and require further validation (Fig. 5A,B). Overall, these data indicate that an increase in LST score and genomic instability emerge following treatment with abiraterone or enzalutamide, but not taxane, and this is associated with *RB1* genomic locus loss with and without *BRCA2* genomic loss, with possible implication of concurrent *RNASEH2B* genomic loss.

4. Discussion

Our data show that the ctDNA fraction obtained via lpWGS provides information regarding prognosis, with serial analyses identifying responding disease. Critically, these assays provide genomic information that can serve as biomarkers of treatment response and detect genomic aberrations and signatures of DNA repair defects [10]. ctDNA lpWGS provides information on emerging mCRPC genomics and can be performed frequently, yielding data for multiple metastatic sites. However, ctDNA assays do have limitations and cannot fully elucidate intrapatient disease heterogeneity; this may be more feasible with analysis of single circulating tumour cells [24].

Interestingly, our study also shows that treatment with abiraterone or enzalutamide is associated with increases in CNAs and LST scores; this was not seen following taxane treatment or radical radiotherapy, and was maintained in the presence of other markers of tumour burden. This suggests differential, therapy-induced, genomic alterations following treatment with next-generation hormonal agents, but not taxanes. Other studies have shown that high LST scores are associated with genomic instability and may be biomarkers for PARP inhibitor sensitivity [12]. We show here that the increase in LST score following treatment with abiraterone or enzalutamide is most associated with loss of loci on chromosome 13, which usually contains the *RB1* and *RNASEH2B* genes, among others. Tumours with loss of *RNASEH2B* have been linked to impaired misincorporated RNA excision from DNA and can sensitise to PARP inhibition [25].

A limitation of ctDNA lpWGS is the fact that plasma samples containing low tumour fractions make precise detection of CNAs, especially subclonal events, challenging [19,26]. A low ctDNA fraction is nevertheless of clinical significance and indicates lower tumour burden and better outcomes. The variation in ctDNA values observed over time may reflect disease behaviour [27]. The ctDNA fraction estimated via lpWGS, unlike cfDNA concentrations [14], is highly correlated with disease response and treatment outcome, probably because a significant proportion of

cfDNA arises from nontumour sources [28,29]. Our observations support the proposal that changes in the ctDNA fraction can track treatment response, and we welcome further exploration of this phenomenon [30,31].

This study may be biased by sample selection; not all patients consented to blood sample donation for these analyses and our analyses focused on patients with available plasma with higher ctDNA levels, which may represent a poor-prognosis cohort. However, there were no statistically significant differences in the response rate or survival between our cohort and the overall trial populations. mCRPCs overall do have some of the highest quantities of cfDNA among adult solid tumour types, making these studies especially useful [32]. This study supports complementary research on ctDNA lpWGS and targeted next-generation sequencing, which together can transform disease management. Further studies to critically validate the prognostic capability of the ctDNA fraction in mCRPC are now necessary, especially in the context of existing validated biomarkers.

5. Conclusions

In conclusion, we demonstrated that cfDNA lpWGS can describe CRPC behaviour, provide prognostic and response data of clinical relevance, and identify emerging genomic alterations that might serve as therapeutic targets.

Appendix A. Supplementary data

Supplementary material related to this article can be found, in the online version, at doi:https://doi.org/10.1016/j.eururo.2021.05.030.

References

[1] Siegel RL, Miller KD, Jemal A. Cancer statistics, 2019. CA Cancer J Clin 2019;69:7–34.

[2] Sartor O, de Bono JS. Metastatic prostate cancer. N Engl J Med 2018;378:645–57.

[3] Tannock IF, de Wit R, Berry WR, et al. Docetaxel plus prednisone or mitoxantrone plus prednisone for advanced prostate cancer. N Engl J Med 2004;351:1502–12.

[4] Berthold DR, Pond GR, Soban F, de Wit R, Eisenberger M, Tannock IF. Docetaxel plus prednisone or mitoxantrone plus prednisone for advanced prostate cancer: updated survival in the TAX 327 study. J Clin Oncol 2008;26:242–5.

[5] Mehra N, Dolling D, Sumanasuriya S, et al. Plasma cell-free DNA concentration and outcomes from taxane therapy in metastatic castration-resistant prostate cancer from two phase III trials (FIRST-ANA and PROSELICA). Eur Urol 2018;74:283–91.

[6] Annala M, Vandekerkhove G, Khalaf D, et al. Circulating tumor DNA genomics correlate with resistance to abiraterone and enzalutamide in prostate cancer. Cancer Discov 2018;8:444–57.

[7] Goodall J, Mateo J, Yuan W, et al. Circulating cell-free DNA to guide prostate cancer treatment with PARP inhibition. Cancer Discov 2017;7:1006–17.

[8] Ulz P, Belic J, Graf R, et al. Whole-genome plasma sequencing reveals focal amplifications as a driving force in metastatic prostate cancer. Nat Commun 2016;7:12008.

[9] Hieronymus H, Schultz N, Gopalan A, et al. Copy number alteration burden predicts prostate cancer relapse. Proc Natl Acad Sci U S A 2014;111:11139–44.

[10] Wu Y-M, Cieślik M, Lonigro RJ, et al. Inactivation of CDK12 delineates a distinct immunogenic class of advanced prostate cancer. Cell 2018;173, 1770–82.e14.

[11] Telli ML, Timms KM, Reid J, et al. Homologous recombination deficiency (HRD) score predicts response to platinum-containing neoadjuvant chemotherapy in patients with triple-negative breast cancer. Clin Cancer Res 2016;22:3764–73.

[12] Jiang X, Li X, Li W, Bai H, Zhang Z. PARP inhibitors in ovarian cancer: sensitivity prediction and resistance mechanisms. J Cell Mol Med 2019;23:2303–13.

[13] Oudard S, Fizazi K, Sengeløv L, et al. Cabazitaxel versus docetaxel as first-line therapy for patients with metastatic castration-resistant prostate cancer: a randomized phase III trial—FIRSTANA. J Clin Oncol 2017;35:3189–97.

[14] Eisenberger M, Hardy-Bessard A-C, Kim CS, et al. Phase III study comparing a reduced dose of cabazitaxel (20 mg/m^2) and the currently approved dose (25 mg/m^2) in postdocetaxel patients with metastatic castration-resistant prostate cancer—PROSELICA. J Clin Oncol 2017;35:3198–206.

[15] Scher HI, Halabi S, Tannock I, et al. Design and end points of clinical trials for patients with progressive prostate cancer and castrate levels of testosterone: recommendations of the Prostate Cancer Clinical Trials Working Group. J Clin Oncol 2008;26:1148–59.

[16] Mateo J, Seed G, Bertan C, et al. Genomics of lethal prostate cancer at diagnosis and castration resistance. J Clin Invest 2020;130:1743–51.

[17] Taylor AC. Titration of heparinase for removal of the PCR-inhibitory effect of heparin in DNA samples. Mol Ecol 1997;6:383–5.

[18] Mateo J, Carreira S, Sandhu S, et al. DNA-repair defects and olaparib in metastatic prostate cancer. N Engl J Med 2015;373:1697–708.

[19] Adalsteinsson VA, Ha G, Freeman SS, et al. Scalable whole-exome sequencing of cell-free DNA reveals high concordance with metastatic tumors. Nat Commun 2017;8:1324.

[20] Marquard AM, Eklund AC, Joshi T, et al. Pan-cancer analysis of genomic scar signatures associated with homologous recombination deficiency suggests novel indications for existing cancer drugs. Biomark Res 2015;3:9.

[21] Candia J, Tsang JS. ENetXplorer: an R package for the quantitative exploration of elastic net families for generalized linear models. BMC Bioinformatics 2019;20:189.

[22] Popova T, Manié E, Rieunier G, et al. Ploidy and large-scale genomic instability consistently identify basal-like breast carcinomas with BRCA1/2 inactivation. Cancer Res 2012;72:5454–62.

[23] Robinson D, Van Allen EM, Wu YM, et al. Integrative clinical genomics of advanced prostate cancer. Cell 2015;161:1215–28.

[24] Lambros MB, Seed G, Sumanasuriya S, et al. Single-cell analyses of prostate cancer liquid biopsies acquired by apheresis. Clin Cancer Res 2018;24:5635–44.

[25] Zimmermann M, Murina O, Reijns MAM, et al. CRISPR screens identify genomic ribonucleotides as a source of PARP-trapping lesions. Nature 2018;559:285–9.

[26] Johansson G, Andersson D, Filges S, et al. Considerations and quality controls when analyzing cell-free tumor DNA. Biomol Detect Quantif 2019;17:100078.

[27] Bromberg JS, Brennan DC, Poggio E, et al. Biological variation of donor-derived cell-free DNA in renal transplant recipients: clinical implications. J Appl Lab Med 2017;2:309–21.

[28] Aucamp J, Bronkhorst AJ, Badenhorst CPS, Pretorius PJ. The diverse origins of circulating cell-free DNA in the human body: a critical re-evaluation of the literature. Biol Rev 2018;93:1649–83.

[29] Bronkhorst AJ, Ungerer V, Holdenrieder S. The emerging role of cell-free DNA as a molecular marker for cancer management. Biomol Detect Quantif 2019;17:100087.

[30] Nygaard AD, Holdgaard PC, Spindler KLG, Pallisgaard N, Jakobsen A. The correlation between cell-free DNA and tumour burden was estimated by PET/CT in patients with advanced NSCLC. Br J Cancer 2014;110:363–8.

[31] Valpione S, Gremel G, Mundra P, et al. Plasma total cell-free DNA (cfDNA) is a surrogate biomarker for tumour burden and a prognostic biomarker for survival in metastatic melanoma patients. Eur J Cancer 2018;88:1–9.

[32] Perkins G, Yap TA, Pope L, et al. Multi-purpose utility of circulating plasma DNA testing in patients with advanced cancers. PLoS One 2012;7:e47020.

[33] Li H, Durbin R. Fast and accurate short read alignment with Burrows-Wheeler transform. Bioinformatics 2009;25(14):1754–60. http://dx.doi.org/10.1093/bioinformatics/btp324, In press.

[35] Lai D, Ha G, Shah S. HMMcopy: Copy number prediction with correction for GC and mappability bias for HTS data. R package 2021. http://dx.doi.org/10.18129/B9.bioc.HMMcopy, In press.